Published in final edited form as:
Reproduction. 2009 September ; 138(3): 463–470. doi:10.1530/REP-09-0201.

Adenine nucleotide translocase 4 deficiency leads to early meiotic arrest of murine male germ cells

Jeffrey V Brower[1], **Chae Ho Lim**[1], **Marda Jorgensen**[1], **S Paul Oh**[2], and **Naohiro Terada**[1]

[1]Department of Pathology, University of Florida College of Medicine, PO Box 100275, Gainesville, Florida 32610, USA

[2]Department of Physiology, University of Florida College of Medicine, PO Box 100275, Gainesville, Florida 32610, USA

Abstract

Male fertility relies on the highly specialized process of spermatogenesis to continually renew the supply of spermatozoa necessary for reproduction. Central to this unique process is meiosis that is responsible for the production of haploid spermatozoa as well as for generating genetic diversity. During meiosis I, there is a dramatic increase in the number of mitochondria present within the developing spermatocytes, suggesting an increased necessity for ATP production and utilization. Essential for the utilization of ATP is the translocation of ADP and ATP across the inner mitochondrial membrane, which is mediated by the adenine nucleotide translocases (Ant). We recently identified and characterized a novel testis specific Ant, ANT4 (also known as SLC25A31 and Aac4). The generation of *Ant4*-deficient animals resulted in the severe disruption of the seminiferous epithelium with an apparent spermatocytic arrest of the germ cell population. In the present study utilizing a chromosomal spread technique, we determined that *Ant4*-deficiency results in an accumulation of leptotene spermatocytes, a decrease in pachytene spermatocytes, and an absence of diplotene spermatocytes, indicating early meiotic arrest. Furthermore, the chromosomes of *Ant4*-deficient pachytene spermatocyte occasionally demonstrated sustained γH2AX association as well as synaptonemal complex protein 1 (SYCP1)/SYCP3 dissociation beyond the sex body. Large ATP supplies from mitochondria may be critical for normal progression of spermatogenesis during early stages of meiotic prophase I, including DNA double-strand break repair and chromosomal synapsis.

Introduction

Spermatogenesis is a highly complex cell differentiation process necessary for continued renewal of the spermatozoa population. Central to this unique process is meiosis, which is responsible for the production of haploid spermatozoa as well as for generating genetic diversity. Meiosis I is initiated in the primary spermatocytes and like mitosis, is separated into interphase, pro-phase, metaphase, anaphase, and telophase (Petronczki *et al*. 2003, Raven *et al*. 2008). During interphase the chromosomes replicate, prior to prophase I. Prophase I of meiosis I is unique in that it is elongated and further broken down into leptotene, zygotene, pachytene, diplotene, and diakinesis (Petronczki *et al*. 2003, Griffiths *et al*. 2005). During these substages of prophase I, the chromosomes undergo a number of changes that allow for the pairing of homologs and the exchange of genetic information

Correspondence should be addressed to N Terada; terada@pathology.ufl.edu.

Declaration of interest

The authors declare that there is no conflict of interest that could be perceived as prejudicing the impartiality of the research reported.

between non-sister chromatids. Briefly, during leptotene the individual chromosomes begin to condense, and during zygotene, homologous chromosomes seek out one another and begin to synapse. This synapsis is mediated through the synaptonemal protein complex (Lammers *et al.* 1994). During this time, γH2AX begins to associate tightly with the X and Y chromosomes. During subsequent pachytene stage, complete condensation and synapsis occurs and genetic diversity is generated by the random process of genetic exchange that occurs between non-sister chromatids of homologous chromosomes. During this time, the sex body is located at the periphery of the nucleus and stains very intensely with γH2AX (Handel 2004). Following the pachytene stage, primary spermatocytes complete the remaining stages of prophase I and subsequent meta-phase, anaphase, and telophase.

The meiotic processes are considered to be highly energy dependent and require a continuous supply of large amounts of ATP (Saunders *et al.* 1993, Meinhardt *et al.* 1999). Of interest, as spermatogonial cells transition into primary spermatocytes they traverse the Sertoli cell-mediated blood–testis barrier, which results in a dramatic change in the microenvironment in which they are immersed (Saunders *et al.* 1993, Meinhardt *et al.* 1999, Chiarini-Garcia *et al.* 2003). Owing to their location beyond the blood–testis barrier, spermatocytes receive metabolites, which provide less energy than glucose, such as lactate. The germ cells that are adluminal to the blood–testis barrier, rely on the breakdown of lactate and pyruvate provided by the Sertoli cells (Grootegoed *et al.* 1984). Indeed, primary rat pachytene spermatocytes in culture utilize lactate and pyruvate much more efficiently than glucose and fructose to maintain ATP levels (Nakamura *et al.* 1984). Furthermore, because of the greater oxygen diffusion distance, the adluminal regions of the seminiferous epithelium are likely to be more hypoxic in comparison with the basal compartments where spermatogonial self-renewal occurs (Marti *et al.* 2002). Thus, despite their high ATP demand, meiotic spermatocytes are probably subject to somewhat harsh conditions for energy production, i.e. lower glucose and lower oxygen.

How then do meiotic spermatocytes cope with this dilemma? Previous studies have recognized the mitochondrial changes in morphology, organization, and number that occur during spermatogenesis and spermiogenesis (Machado de Domenech *et al.* 1972, Stefanini *et al.* 1974, De Martino *et al.* 1979, Meinhardt *et al.* 1999). In type A spermatogonia, the mitochondria are orthodox in morphology, being ovoid in shape and containing lamellar cristae (Stefanini *et al.* 1974). In type B spermatogonia, the intracristal space begins to dilate, which becomes more apparent during the transition to leptotene primary spermatocytes (Meinhardt *et al.* 1999). During zygotene and early pachytene stages, the mitochondria elongate and associate with the outer nuclear membrane as their numbers steadily increase. These studies indicate the active functional status of the mitochondria in developing spermatocytes (Stefanini *et al.* 1974). Functional studies on rat diplotene primary spermatocytes and secondary spermatocytes showed remarkably high respiratory control ratios and very high affinities for ADP as demonstrated by their low K_m values (De Martino *et al.* 1979). These biochemical findings also suggest a high oxidative capacity in spermatocytes (De Martino *et al.* 1979). Furthermore, a recent study demonstrated that the accumulation of mitochondrial DNA mutations affecting mitochondrial respiration resulted in the arrest of spermatocytes primarily at the zygotene stage (Nakada *et al.* 2006). Taken together, these studies indicate that meiotic progression in spermatocytes is particularly sensitive to any reduction in the respiratory function of mitochondria.

Thus, efficient ATP production through oxidative phosphorylation appears to be a key adaptation in the successful progression of meiotic spermatocytes. However, for utilization of ATP, mitochondrial ATP must be carried out of the mitochondrial matrix to the intermembrane space through the adenine nucleotide translocase (Ant, also called ADP/ATP carrier, Aac) and subsequently allowed to diffuse into the cytoplasm (Gawaz *et al.* 1990,

Fiore *et al*. 1998, Levy *et al*. 2000, Dolce *et al*. 2005, Rodic *et al*. 2005, Brower *et al*. 2007). We and others recently identified a novel mammalian Ant, ANT4 (also called SLC25A31, Aac4), which may be responsible for ADP/ATP exchange particularly during spermatogenesis (Dolce *et al*. 2005, Rodic *et al*. 2005, Brower *et al*. 2007, Kim *et al*. 2007). Of interest, disruption of the *Ant4* gene in mice led to a complete loss of male fertility (Brower *et al*. 2007). The *Ant4*-deficient males exhibited increased levels of apoptosis within the spermatocyte layer of the seminiferous epithelium, accompanied by the absence of spermatids and spermatozoa within the seminiferous epithelium and lumen respectively (Brower *et al*. 2007). In order to obtain further insight regarding the role of ANT4 during spermatogenesis, the present study attempted to determine the precise stage at which *Ant4*-deficient spermatocytes undergo arrest.

Results

Ant4-deficient testes possess a greater proportion of early stage spermatocytes

In order to determine the stage of meiosis I during which *Ant4*-deficient spermatocytes undergo arrest, we initially performed immunohistochemical analysis investigating synaptonemal complex protein 3 (SYCP3) expression. SYCP3 is a component of the lateral elements of synaptonemal complexes and is thus present only during meiosis I (Lammers *et al*. 1994). Testicular cross-sections of *Ant4*-deficient mice were stained with anti-SYCP3 antibody and compared with *Ant4* wild-type testicular preparations (Fig. 1). Counter staining with hematoxylin allowed for visualization of the nuclear morphology of cells within seminiferous tubules of wild-type and *Ant4*-deficient testes. As we previously described (Brower *et al*. 2007), *Ant4*-deficient testes demonstrated impaired completion of spermatogenesis, having no apparent spermatids or mature sperm in the tubules.

SYCP3 staining of wild-type testis at low magnification demonstrated spermatocyte-specific staining of SYCP3 as shown by the clearly identifiable ring of spermatocytes present one step adluminal to the spermatogonial cells located along the basal lamina. Observation of SYCP3 staining at low magnification allowed us to confirm the presence of primary spermatocytes within the *Ant4*-deficient testis, which was consistent with the RNA expression profile data regarding the population of cells present within the seminiferous epithelium of *Ant4*-deficient testis (Brower *et al*. 2007). After determining that *Ant4*-deficient testis indeed possessed spermatocytes we sought to investigate, which stages of spermatocytes were present. Upon closer analysis at higher magnification, the wild-type spermatocytic compartment contained a greater proportion of spermatocytes with more highly condensed nuclei. These spermatocytes exhibiting a greater extent of nuclear condensation are representative of later stage, zygotene-to-pachytene-like spermatocytes (Peters *et al*. 1997). In contrast to the wild-type spermatocytes, *Ant4*-deficient testis possessed a dominant proportion of spermatocytes with a lesser degree of nuclear condensation, suggestive of early stage, leptotene-like spermatocytes. It is important to note that *Ant4*-deficient testis did, however, possess what appeared to be zygotene or pachytene spermatocytes (indicated by arrow heads in Fig. 1).

Ant4-deficient testes exhibit a failure to complete meiosis I as evidenced by the absence of diplotene spermatocytes

The initial staining of testicular cross sections with SYCP3 allowed us to determine that there was an accumulation of early spermatocytes in the *Ant4*-deficient testis. In order to more precisely determine the stage of meiotic arrest in *Ant4*-deficient mice, we utilized a chromosomal spread technique. This technique allowed us to analyze the exact chromosomal status of the spermatocyte being investigated at the single-cell level and thus determine its stage. In order to investigate the specific stages of spermatocytes present

within the *Ant4*-deficient testicular preparations in comparison with wild-type controls, we utilized SYCP3, γH2AX, and DAPI staining. DAPI stains double-strand DNA and was utilized for the identification of various cell types based upon nuclear morphology. DAPI staining also makes it possible to visualize the chromosomal condensation status of the cells being investigated. SYCP3 staining was utilized primarily to determine the staging of the prophase I spermatocytes, as SYCP3 associates with the chromosomes from leptotene through diplotene and allows us to visualize the chromosomal changes that define the different stages (Peters *et al.* 1997). γH2AX is known to diffusely associate with the chromosomes during the leptotene stage, and exclusively associates with the XY body within pachytene and diplotene spermatocytes (Peters *et al.* 1997, Celeste *et al.* 2002).

Analysis of wild-types permatocytes showed the presence of leptotene through diplotene spermatocytes (Fig. 2A). The leptotene spermatocytes demonstrated a diffuse DAPI nuclear staining as well as punctate staining of both γH2AX and SYCP3 throughout the chromosomes. The zygotene spermatocytes showed increased nuclear condensation as visualized by DAPI and SYCP3 staining. γH2AX began to associate with the X and Y chromosomes as the sex body began to form during the zygotene stage. Pachytene spermatocytes were easily distinguished through SYCP3 staining by the delineation of highly condensed, synapsed, and homologous chromosome pairs. A highly condensed γH2AX positive sex body located at the periphery of the nucleus also confirmed the presence of pachytene spermatocytes. Diplotene spermatocytes also demonstrated highly condensed chromosomes and distinct sex bodies but were distinguishable from pachytene spermatocytes by the presence of chiasmata with the separation of homologous chromosome pairs, which was visualized by SYCP3 staining.

The analysis of *Ant4*-deficient spermatocytes demonstrated the presence of apparently normal leptotene spermatocytes as evidenced by the diffuse nuclear staining of DAPI as well as punctate but diffuse localization of γH2AX and SYCP3 (Fig. 2B). Zygotene spermatocytes also appeared to be normal as the nuclear staining of DAPI showed regions of increased condensation. Also, γH2AX staining coincided with the beginning stage of sex body formation. Consistent with the apparent normal presence of zygotene spermatocytes in the *Ant4*-deficient testis was the increased condensation of the chromosomes as shown by SYCP3 staining. Pachytene spermatocytes, as identified by highly condensed and synapsed chromosome pairs, were present within *Ant4*-deficient testis. However, no apparent diplotene primary spermatocytes were observed in the *Ant4*-deficient testis.

Ant4-deficient testes exhibit early meiotic arrest

In order to determine the stage of arrest of the spermatocytic populations in *Ant4*-deficient testis, we carried out a quantification analysis. Approximately 500 spermatocytes were counted in both the $Ant4^{+/+}$ and $Ant4^{-/-}$ spermatocytic preparations. The stage of prophase I for each spermatocyte was then determined by chromosomal morphology analysis and sex body status. The *Ant4* wild-type testis contained a normal distribution of spermatocytes with the largest percentage being present within pachytene (56%), followed by zygotene (22%), diplotene (15%), and leptotene (7%; Fig. 3). The spermatocytic quantification demonstrated a significant redistribution of the spermatocyte population in *Ant4*-deficient preparations with the largest percentage being present within leptotene (66%), followed by zygotene (26%), and pachytene (8%) respectively (Fig. 4). These data demonstrate that in the *Ant4*-deficient testis there is an accumulation of leptotene spermatocytes with a significant decrease in the percentage of pachytene, and an absence of diplotene spermatocytes. These data were consistent with the observations obtained by SYCP3 immunohistochemistry (Fig. 1).

Abnormal gH2AX association and SYCP1/SYCP3 dissociation in *Ant4*-deficient pachytene spermatocytes

Although pachytene spermatocytes were present in the *Ant4*-deficient testis, significant abnormalities in γH2AX staining were observed. The abnormalities ranged from what appeared to be improper and diffuse localization of γH2AX beyond sex bodies (Fig. 2C, left and center panels), to possible telomeric localization of γH2AX (Fig. 2C, right panel). Approximately half (45/100) of the *Ant4*-deficient pachytene spermatocytes exhibited some type of aberrant γH2AX localization and condensation, whereas none (0/100) showed such abnormalities in wild-type spermatocytes. We further investigated potential abnormal synapsis in pachytene spermatocytes by co-staining with SYCP1 (a central element protein) and SYCP3 (a lateral element protein). As shown in Fig. 4, all the pachytene spermatocytes (34/34) in wild-type testis demonstrated a complete alignment of SYCP1 and SYCP3, except at apparent sex bodies where unpaired XY chromosomes lack the central element (SYCP1; Fig. 4, upper panels). In the *Ant4*-deficient pachytene spermatocytes, the majority of cells (32/42) also exhibited apparent normal synapsis (Fig. 4, middle panels). However, roughly a quarter of the cells (10/42) exhibited additional chromosome sites lacking SYCP1 staining, indicating the existence of aberrant asynapsis in the autosomes (Fig. 4, lower panels).

Discussion

In the previous study, we demonstrated that ablation of the *Ant4* gene, which is considered to be necessary for the translocation of ATP from the mitochondrial matrix into the cytosol within testicular germ cells, resulted in severe disruption of the seminiferous epithelium and subsequent male infertility. In the present study, we sought to further elucidate the function of ANT4 during spermatogenesis by determining the exact stage during meiosis that *Ant4*-deficient spermatocytes arrest. We found *Ant4*-deficiency resulted in the complete absence of diplotene spermatocytes, whereas the wild-type mice display an apparently normal proportion of diplotene spermatocytes. Further disruption of *Ant4* resulted in a severe reduction in the percentage of pachytene spermatocytes in comparison with wild-type controls. We also found an accumulation of leptotene spermatocytes upon *Ant4* disruption without a significant change in the proportion of zygotene spermatocytes. These data taken together suggest that *Ant4* deficiency impairs the progression of male meiosis, and that this impairment becomes most evident at the transition from leptotene to zygotene stage. Of interest, the meiotic arrest phenotype here is similar, but not identical, to that caused by mitochondrial DNA mutation (Nakada *et al.* 2006). The *Ant4*-deficiency resulted in an arrest of spermatocytes predominantly at the leptotene stage, whereas mitochondrial DNA mutation resulted in an arrest predominantly at the zygotene stage. This discrepancy might be explained by differences in the severity of ATP depletion in two mice models. *Ant4*-deficiency would lead to a complete shutdown of ATP supplies from mitochondria in male germ cells (Brower *et al.* 2007). These two studies taken together, however, indicate that early prophase I stages are particularly sensitive to reduced levels of respiration and subsequent ATP availability within the cell, supporting the idea that ATP production via oxidative phosphorylation is essential for the meiotic progression of spermatocytes. It should be noted that this is in contrast with some of the downstream events in spermatogenesis such as sperm capacitation, motility changes, acrosome reaction, and fertilization,which can depend exclusively upon glycolysis and can occur under strictly anaerobic conditions (Fraser & Quinn 1981, Welch *et al.* 2000).

Interestingly, in addition to a decrease in number, many *Ant4*-deficient pachytene spermatocytes displayed abnormalities in chromatid organization, condensation, and synapsis. γH2AX was often associated outside of apparent sex bodies in *Ant4*-deficient pachytene cells, suggesting that unrepaired DNA double-strand breaks may remain in these

cells. Furthermore, our data also indicate that incomplete chromosomal synapsis exists at least in some pachytene spermatocytes. Such abnormalities would be recognized by the pachytene checkpoint (Roeder & Bailis 2000), and eventually the cells would be eliminated. Indeed, we previously demonstrated increased apoptosis in *Ant4*-deficient spermatocytes, consistent with the current observation (Brower *et al.* 2007).

In summary, the present data define an essential role for ANT4 in murine meiotic progression, more specifically in supporting the increased dependency of early stage spermatocytes on ADP/ATP exchange. Sufficient ATP supplies from mitochondria may be important for repair of DNA double-strand breaks as well as chromosomal synapsis during prophase I. This work provides further insight into the specific metabolic requirements of meiotic spermatocytes, indicating that regardless of suggestions that the adluminal compartment is more hypoxic, the spermatocytes within it still depend highly upon the oxidative processes of respiration. It is possible that ANT4 may have developed as a more efficient ADP/ATP exchanger specialized for the unique hypoxic conditions present within the adluminal compartment of the seminiferous epithelium. In addition, independent of the present study, ANT4 is likely the predominant Ant in spermatozoa (Brower *et al.* 2007). This may suggest a specialized adaptation of ANT4 in order to support sperm motility (Kim *et al.* 2007). Future biochemical analysis of ANT4 as well as the development of animals with replacement of ANT4 with somatic Ants (ANT1 or ANT2) may provide us with further insight.

Materials and Methods

Animals and tissues

A mouse line carrying the targeted disruption of the *Ant4* gene (Brower *et al.* 2007) was maintained in a C57BL/6J×129/SV mixed background by mating homozygous ($Ant4^{-/-}$) females with heterozygous ($Ant4^{+/-}$) males. Genotyping was carried out by PCR analysis of genomic DNA as we previously described (Brower *et al.* 2007). Dissected testes for chromosomal spread preparations were used immediately after removal. Tissues for immunohistochemical studies were fixed in 3.7% formaldehyde in PBS overnight at 4 °C. All mice have been maintained under standard-specific pathogen-free conditions, and the procedures performed on the mice were reviewed and approved by the University of Florida Institutional Animal Care and Use Committee.

Immunostaining

The mice utilized for immunohistochemical analysis were age-matched littermates (~6 weeks). Deparaffinized and re-hydrated 5 μm tissue sections were stained with rabbit anti-Sycp3 antibody (Ab15092, Abcam, Cambridge, MA, USA). Slides were blocked for endogenous peroxidase activity and then unmasked in Target Retrieval Solution (DakoCytomation, Carpinteria, CA, USA). Antibody was applied at 1:200 for 1 h at room temperature prior to identification with an anti-rabbit detection kit using DAB (diaminobenzidine; Envision^{+}, Dakocytomation). An isotype and concentration matched negative control section was included for each tissue. Slides were counterstained with hematoxylin.

Meiotic chromosomal spread analysis

Meiotic chromosomal spreads were prepared using a protocol similar to those previously described (Peters *et al.* 1997, Nickerson *et al.* 2007). Briefly, testes were freshly dissected from adult mice (6 weeks) and decapsulated. Tunica albuginea and extratubular tissue were removed by rinsing the seminiferous tubules in PBS. The tubules were then blotted dry to remove excess PBS and placed in hypotonic extraction buffer (30 mM Tris, 50 mM sucrose,

17 mM trisodium citrate dehydrate, 5 mM EDTA, 0.5 mM phenylmethylsulphonyl fluoride, pH 8.2) for 30–50 min. The tubules were gently inverted periodically during the incubation. Following incubation in hypotonic extraction buffer, one-inch lengths of tubules were placed in 20 μl sucrose solution (100 mM sucrose, adjusted with NaOH to pH 8.2) and torn into small pieces with fine forceps. The volume was then increased to 40 μl with sucrose solution and pipetted to give a cloudy suspension. The cell suspension was spread onto two slides dipped in formaldehyde solution (1% formaldehyde, 0.15% Triton X-100 in water adjusted with sodium borate to pH 9.2). It is crucial to make the formaldehyde solution fresh before each experiment, as the pH will change if the solution is left to sit for too long. Slides were then placed in humidified chambers for 2 and 3 h to allow for partial drying of the slides. Slides were then allowed to air-dry at room temperature for approximately an hour or until slides were visibly dry. The slides were either used immediately or stored at −20 °C. For immunostaining, slides were rinsed for 5 min in PBS and then incubated for 30 min in wash/dilution buffer (3% BSA, 0.5% Triton X-100 in PBS). This protocol was adapted from Nickerson *et al.* (2007). Spermatocytic preparations were incubated with both rabbit polyclonal anti-Sycp3 (Ab15092, Abcam) and mouse monoclonal anti-γH2AX (Ab22551, Abcam) antibodies at 1:200 dilutions in wash/dilution buffer and incubated at 4 °C overnight. Following three 3-min washes in PBS, fluorescent conjugated secondary antibody, diluted 1:2000 in wash/dilution buffer, were added and incubated for 45 min at room temperature in the dark. SYCP3 staining was visualized with an Alexa-fluor 488-conjugated anti-rabbit IgG antibody and γH2AX was visualized with a Cy3-conjugated anti-mouse IgG antibody. In other experiments, spermatocytic preparations were stained with goat polyclonal anti-SYCP3 (sc-20845; Santa Cruz Bio-technology, Santa Cruz, CA, USA) and rabbit polyclonal anti-SYCP1 (Ab15090, Abcam) antibodies at 1:200 dilutions, followed by Alexa-fluor 568-conjugated anti-goat IgG antibody and Alexa-fluor 488-conjugated anti-rabbit IgG antibody at 1:500 dilutions. Slides were then washed in PBS, stained, and mounted with Vectashield (Vector Laboratories, Inc., Burlingame, CA, USA) containing DAPI. DAPI was added to slides to visualize DNA.

Acknowledgments

Funding

This work was supported in part by NIH grants U01HD060474 to N Terada.

We thank Dr J L Resnick (U Florida) and members of Terada's lab for critical reading of the manuscript.

References

Brower JV, Rodic N, Seki T, Jorgensen M, Fliess N, Yachnis AT, McCarrey JR, Oh SP, Terada N. Evolutionarily conserved mammalian adenine nucleotide translocase 4 is essential for spermatogenesis. Journal of Biological Chemistry. 2007; 282:29658–29666. [PubMed: 17681941]

Celeste A, Petersen S, Romanienko PJ, Fernandez-Capetillo O, Chen HT, Sedelnikova OA, Reina-San-Martin B, Coppola V, Meffre E, Difilippantonio MJ, et al. Genomic instability in mice lacking histone H2AX. Science. 2002; 296:922–927. [PubMed: 11934988]

Chiarini-Garcia H, Raymer AM, Russel LD. Non-random distribution of spermatogonia in rats: evidence of niches in the seminiferous tubules. Reproduction. 2003; 126:669–680. [PubMed: 14611641]

Dolce V, Scarcia P, Lacopetta D, Palmieri F. A fourth ADP/ATP carrier isoform in man: identification, bacterial expression, functional characterization and tissue distribution. FEBS Letters. 2005; 579:633–637. [PubMed: 15670820]

Fiore C, Trézéguet V, Le Saux A, Roux P, Schwimmer C, Dianoux AC, Noél F, Lauquin GJ, Brandolin G, Vignais PV. The mitochondrial ADP/ATP carrier: structural, physiological and pathological aspects. Biochimie. 1998; 80:137–150. [PubMed: 9587671]

Fraser LR, Quinn PJ. A glycolytic product is obligatory for initiation of the sperm acrosome reaction and whiplash motility required for fertilization in the mouse. Journal of Reproduction and Fertility. 1981; 61:25–35. [PubMed: 7452624]

Gawaz M, Douglas MG, Klingenberg M. Structure–function studies of adenine nucleotide transport in mitochondria. Journal of Biological Chemistry. 1990; 265:14202–14208. [PubMed: 2167309]

Griffiths, AJF.; Wessler, SR.; Lewontin, RC.; Gelbart, WM.; Suzuki, DT.; Miller, JH. An Introduction to Genetic Analysis. 8. New York, NY, USA: W.H. Freeman; 2005. Mitosis and meiosis; p. 782

Grootegoed JA, Jansen R, Van der Molen HJ. The role of glucose, pyruvate and lactate in ATP production by rat spermatocytes and spermatids. Biochimica et Biophysica Acta. 1984; 767:248–256. [PubMed: 6498180]

Handel MA. The XY body: a specialized meiotic chromatin domain. Experimental Cell Research. 2004; 296:57–63. [PubMed: 15120994]

Kim YH, Haidl G, Schaefer M, Egner U, Herr JC. Compartmentalization of a unique ADP/ATP carrier protein SFEC (sperm flagellar energy carrier, AAC4) with glycolytic enzymes in the fibrous sheath of the human sperm flagellar principal piece. Developmental Biology. 2007; 302:463–476. [PubMed: 17137571]

Lammers JH, Offenberg HH, van Aalderen M, Vink AC, Dietrich AJ, Heyting C. The gene encoding a major component of the lateral elements of synaptonemal complexes of the rat is related to X-linked lymphocyte-regulated genes. Molecular and Cellular Biology. 1994; 14:1137–1146. [PubMed: 8289794]

Levy SE, Chen Y, Graham BH, Wallace DC. Expression and sequence analysis of the mouse adenine nucleotide translocase 1 and 2 genes. Gene. 2000; 254:57–66. [PubMed: 10974536]

Machado de Domenech E, Domenech CE, Aoki A, Blanco A. Association of the testicular lactate dehydrogenase isozyme with a special type of mitochondria. Biology of Reproduction. 1972; 6:136–147. [PubMed: 5014040]

Marti HH, Katschinski DM, Wagner KF, Schaffer L, Stier B, Wenger RH. Isoform-specific expression of hypoxia-inducible factor-1α during the late stages of mouse spermatogenesis. Molecular Endocrinology. 2002; 16:234–243. [PubMed: 11818497]

De Martino C, Floridi A, Marcante ML, Malorni W, Scorza Barcellona P, Belloci M, Silvestrini B. Morphological, histochemical and biochemical studies on germ cell mitochondria of normal rats. Cell and Tissue Research. 1979; 196:1–22. [PubMed: 421242]

Meinhardt A, Wilhelm B, Seitz J. Expression of mitochondrial marker proteins during spermatogenesis. Human Reproduction Update. 1999; 5:108–119. [PubMed: 10336016]

Nakada K, Sato A, Yoshida K, Morita T, Tanaka H, Inuoe S, Yonekawa H, Hayashi J. Mitochondrial-related male infertility. PNAS. 2006; 103:15148–15153. [PubMed: 17005726]

Nakamura T, Okinaga S, Arai K. Metabolism of pachytene spermatocytes primary spermatocytes from rat testes: pyruvate maintenance of adenosine triphosphate level. Biology of Reproduction. 1984; 30:1187–1197. [PubMed: 6733209]

Nickerson HD, Joshi A, Wolgemuth DJ. Cyclin A-1 deficient mice lack histone H3 serine 10 phosphorylation and exhibit altered aurora B dynamics in late prophase of male meiosis. Developmental Biology. 2007; 306:725–735. [PubMed: 17498682]

Peters AH, Plug AW, van Vugt MJ, de Boer P. A drying-down technique for the spreading of mammalian meiocytes from the male and female germline. Chromosome Research. 1997; 5:66–71. [PubMed: 9088645]

Petronczki M, Siomos MF, Nasmyth K. Un ménage à quatre: the molecular biology of chromosome segregation in meiosis. Cell. 2003; 112:423–440. [PubMed: 12600308]

Raven, PH.; Johnson, GB.; Mason, KA.; Losos, J.; Singer, S. Biology. 8. New York, NY, USA: McGraw-Hill; 2008. Sexual reproduction and meiosis; p. 1259

Rodic N, Oka M, Hamazak T, Murawski MR, Jorgensen M, Maatouk DM, Resnick JL, Li E, Terada N. DNA methylation is required for silencing of ant4, an adenine nucleotide translocase selectively expressed in mouse embryonic stem cells and germ cells. Stem Cells. 2005; 23:93–102. [PubMed: 15625126]

Roeder GS, Bailis JM. The pachytene checkpoint. Trends in Genetics. 2000; 16:395–403. [PubMed: 10973068]

Saunders PTK, Millar MR, West AP, Sharpe RM. Mitochondrial cytochrome C oxidase II messenger ribonucleic acid is expressed in pachytene spermatocytes at high levels and in a stage-dependent manner during spermatogenesis in the rat. Biology of Reproduction. 1993; 48:57–67. [PubMed: 8380346]

Stefanini M, De Martino C, D'Agostino A, Agrestini A, Monesi V. Nucleolar activity of rat primary spermatcoytes. Experimental Cell Research. 1974; 86:166–170. [PubMed: 4831156]

Welch JE, Brown PL, O'Brien DA, Magyar PL, Bunch DO, Mori C, Eddy EM. Human glyceraldehyde 3-phosphate dehydrogenase-2 gene is expressed specifically in spermatogenic cells. Journal of Andrology. 2000; 21:328–338. [PubMed: 10714828]

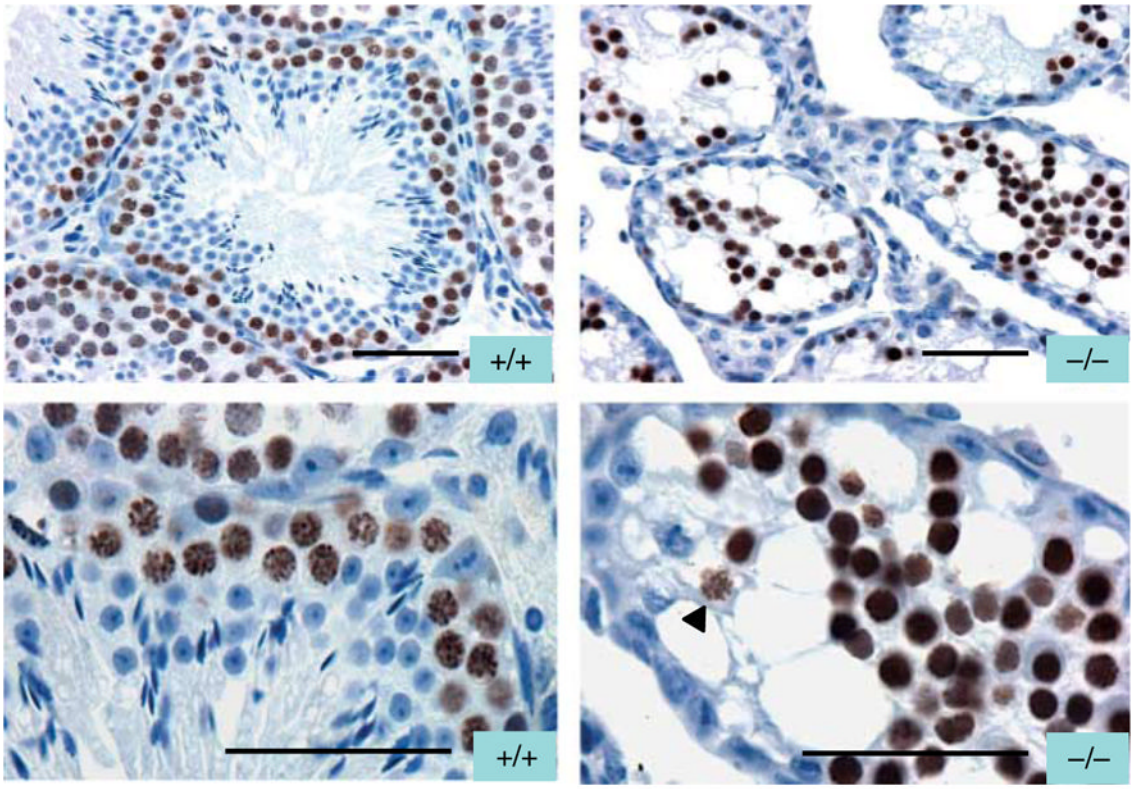

Figure 1.
Immunohistochemical analysis of SYCP3 expression in seminiferous tubules of wild-type and *Ant4*-deficient testes. Formalin-fixed, paraffin-embedded sections of mouse testis from 6-week-old wild-type (+/+) or *Ant4*-deficient (−/−) mice were incubated with rabbit polyclonal antibody against SYCP3. SYCP3 staining was visualized using DAB (brown), and slides were counterstained with hematoxylin. Left panels demonstrate the SYCP3 expression in wild-type testis while right panels show that in *Ant4*-deficient testis. Upper panels and lower panels are low and high magnification images respectively. Scale bars: 50 μm.

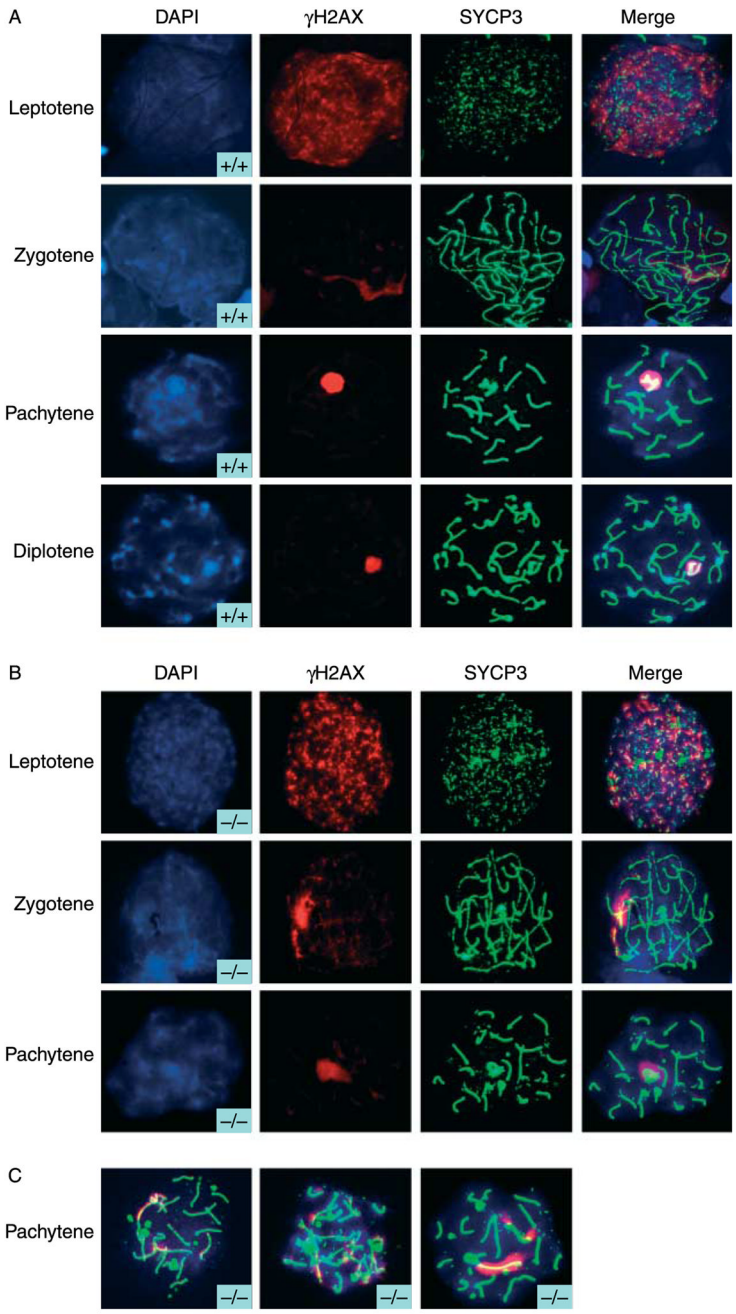

Figure 2.

Chromosomal spread analysis of meiotic spermatocytes from (A) wild-type and (B and C) *Ant4*-deficient testes: SYCP3 and γH2AX staining. Meiotic chromosomal spreads were prepared from freshly dissected testis from 6-week-old wild-type (+/+) and *Ant4*-deficient (−/−) mice as described in Materials and Methods. Spermatocytic preparations were stained with rabbit polyclonal anti-SYCP3 and mouse monoclonal anti-γH2AX antibodies. SYCP3 staining was visualized with an Alexa-fluor 488 conjugated anti-rabbit IgG antibody (green), and γH2AX was visualized with a Cy3 conjugated anti-mouse IgG antibody (red). DNA was counter-stained with DAPI. Representative images of leptotene, zygotene, pachytene, and diplotene spermatocytes isolated from wild-type testis (A) and *Ant4*-deficient testis (B)

are shown. Merged images for representative abnormal pachytene spermatocytes in *Ant4*-deficient testis are shown in (C).

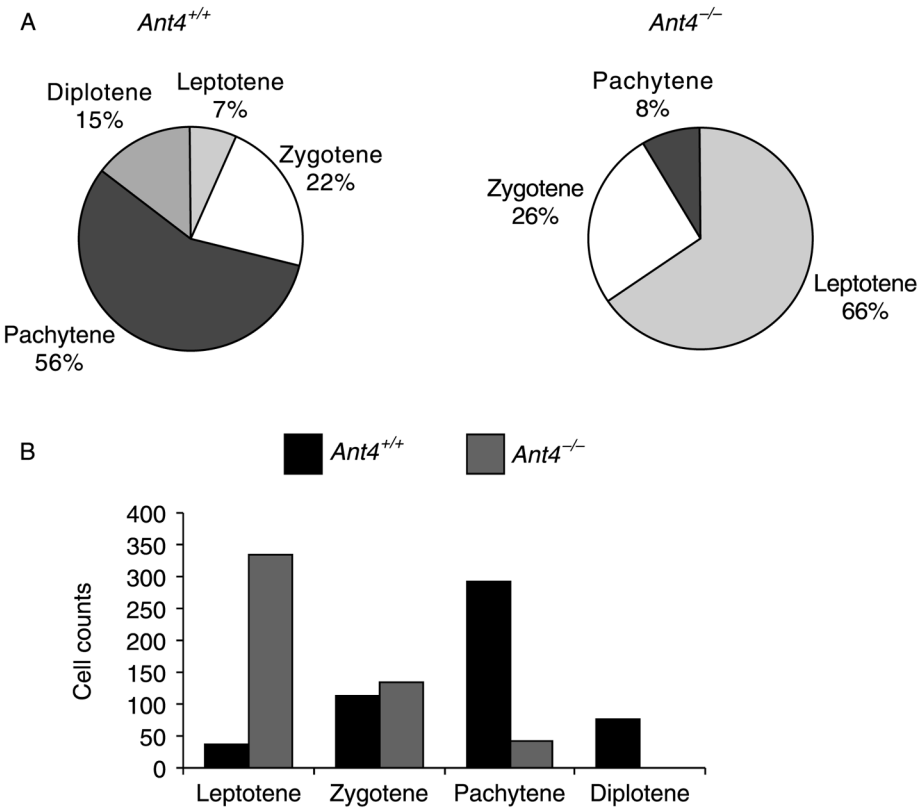

Figure 3.

Distribution of the stage-specific primary spermatocyte population in wild-type and *Ant4*-deficient testes. Meiotic chromosomal spreads were prepared from wild-type (+/+) and *Ant4*-deficient (−/−) mice and stained with anti-SYCP3 and anti-γH2AX antibodies as described in Fig. 2. The number of prophase I spermatocytes at each stage (leptotene, zygotene, pachytene, and diplotene) were counted (total 550 cells per condition). (A) Percentage analysis of the spermatocytic cells present in the seminiferous epithelium of wild-type (+/+) and *Ant4*-deficient (−/−) testes. (B) Bar graph representation of the actual numbers of each spermatocytic stage present in $Ant4^{+/+}$and $Ant4^{-/-}$ mice.

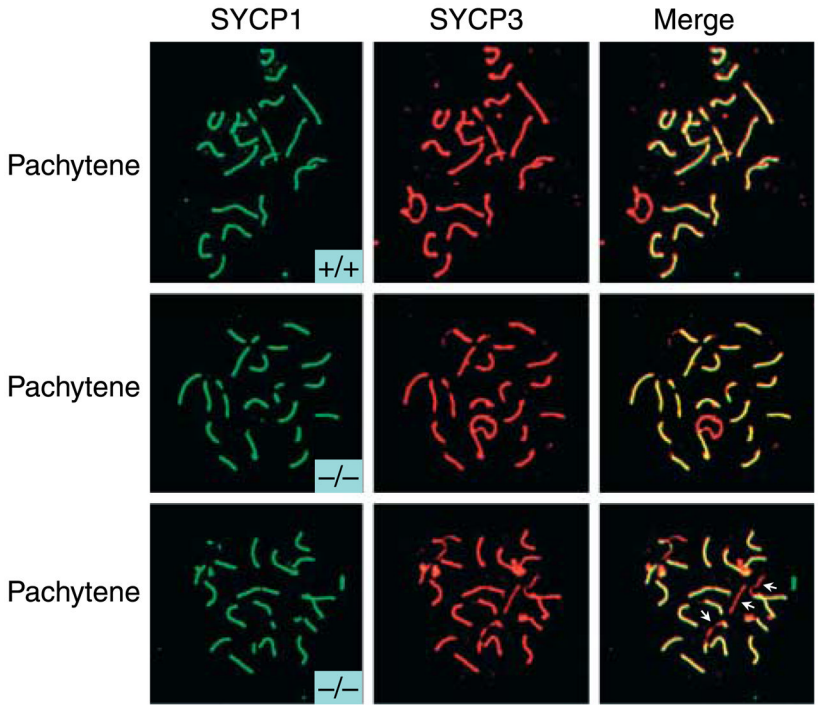

Figure 4.

Chromosomal spread analysis of meiotic spermatocytes from wild-type and *Ant4*-deficient testes: SYCP1 and SYCP3 staining. Meiotic chromosomal spreads were prepared from wild-type (+/+) and *Ant4*-deficient (−/−) mice as described in Fig. 2. Spermatocytic preparations were stained with rabbit polyclonal anti-SYCP1 and goat polyclonal anti-SYCP3 antibodies. SYCP1 was visualized with an Alexa-fluor 488 conjugated anti-rabbit IgG antibody (green), and SYCP3 staining was visualized with an Alexa-fluor 568 conjugated anti-goat IgG antibody (red).